



Repositorio Institucional de la Universidad Autónoma de Madrid

<https://repositorio.uam.es>

Esta es la **versión de autor** del artículo publicado en:

This is an **author produced version** of a paper published in:

Journal of Physical Chemistry C 120.1 (2016): 731-736

DOI: <http://dx.doi.org/10.1021/acs.jpcc.5b10601>

Copyright: © 2015 American Chemical Society

El acceso a la versión del editor puede requerir la suscripción del recurso

Access to the published version may require subscription

Pyroelectric Trapping and Arrangement of Nanoparticles in Lithium Niobate Opposite Domain Structures

*Ana Gallego, Angel García-Cabañes, Mercedes Carrascosa and Luis Arizmendi**

Departamento de Física de Materiales, Universidad Autónoma de Madrid, Avenida Francisco
Tomás y Valiente 7, E28049 Madrid, SPAIN.

ABSTRACT: The particular ferroelectric domain structure of periodic opposite domain lithium niobate (ODLN) crystals has been used for the first time for structured nanoparticle trapping. The surface charge density produced by a temperature change in this pyroelectric material is the origin of the trapping forces: dielectrophoretic on neutral particles and electrophoretic on charged ones. Metallic and dielectric particles are trapped and structured. The results show that ODLN structures are efficient substrates for pyroelectric trapping. The different trapping behaviors are presented.

Keywords: Electrophoresis, Dielectrophoresis, Nanochains, Nanostructures

INTRODUCTION

Nowadays the availability of tools for manipulation of micro and nanoparticles is a key aspect in many fields such as nanotechnology or biomedicine. For this purpose several techniques have been established mainly based on optical (Optical tweezers¹), electrokinetical² or magnetic³ methods. However, for a number of applications massive simultaneous particle manipulation is required. In this case the use of light⁴⁻⁶ or thermally-induced⁷ electric fields generated in certain ferroelectrics have been recently proposed and successfully applied. However, these techniques are still young and new developments and applications are continuously arising^{8,9}.

Among ferroelectrics one of the best candidates for particle manipulation is lithium niobate. It is a ferroelectric material for temperatures below the high Curie point at about 1100°C¹⁰. This property gives rise to the formation of ferroelectric domains or regions of oriented dipoles. Permanent electric dipoles are oriented along the trigonal structural c-axis. Only two domain orientations are possible with the spontaneous polarization P_s vector directed at 180° one to the other. For many applications a single domain material is required. Other domain structures have been produced and advantageously used for other applications¹¹. Particularly, the periodic poled lithium niobate (PPLN) structures consist of arrays of alternate oriented domains with separation walls parallel to the polarization direction. They are obtained either by means of a special crystal growth technique or by a poling process applied to the crystals. Another different periodic domain structure is that where the domain walls are perpendicular to the polarization vector. In this case the domains are oriented “head to head” and “tile to tile”. Walls with positive and negative charge are alternated along the structure. These structures are known as opposite domain lithium niobate (ODLN). ODLN can be obtained by the off-centered Czochralski crystal

growth technique with the addition of impurities such as Y or Er¹². ODLN structures are considered for applications in acoustic wave resonators¹³.

The surface charge density appearing at the end surface of ferroelectric domains is usually compensated in the air by ambient moisture absorbed ions. Temperature dependence of the spontaneous polarization P_s gives rise to the pyroelectric effect¹⁴. A temperature change induces a dipole polarization change which results in the occurrence of a temporary surface charge density at the domain ends. After some time this charge density will be also screened by external charges. If there nanoparticles (NPs) in the vicinity of the material, this screening process can be achieved by trapping of NPs on its surface.

The thermal-induced electrokinetic methods for particle manipulation are just based in these screening processes. They provide a very interesting way for controlled trapping and manipulation of NPs. In principle, the corresponding electro-kinetic forces can act either on charged particles (electrophoresis) or on neutral particles (dielectrophoresis) as extensively discussed in the theoretical work reported by P. Mokry et al.¹⁵. However, previous reported experiments that use pyroelectric generated space-charge distributions on the surface of PPLN structures refer only to dielectrophoresis^{7,8,16}.

In this work we study the capabilities and peculiarities of nanoparticle trapping on ODLN structures by the pyroelectric effect. Up to our knowledge this is the first work dedicated to particle trapping in such a kind of domain structures. Before presenting the trapping results, we will characterize the used ODLN sample.

EXPERIMENTAL METHODS

Characterization of the ODLN sample structure. The sample used in the experiments is a lithium niobate crystal having opposite domain structures. It was grown by the off-centered

Czochralski technique^{12,17}. The starting material was congruent lithium niobate powder with 3 mol% of Er, added to the melt as Er_2O_3 . The pulling direction was along the c-axis of the crystalline seed. From the crystal boule, a 1mm thick plate was cut and polished up to optical grade. The plate faces were perpendicular to the y-axis, therefore the ferroelectric c-axis was contained in the larger faces of the plate.

A first characterization method to reveal the domain structure is chemical etching. LN crystals can be etched by a $\text{HF}:\text{HNO}_3$ (1:2 by vol.) mixture at high temperature. It is well known¹⁸ that the two different domain ends, c+ and c-, have very different etching speed. In fact, the etching speed of negative domain ends is much faster than that of the positive ones. However, in a y-cut sample no domain ends on the surface as the polarization vector \mathbf{P}_s is parallel to the faces. One could expect that the etching speed will be uniform at every point of the face. Nevertheless, this is not right for places where the ODLN domain walls intersect the plate surface. The ODLN domain walls are places of charge accumulation, positive for the “head to head” walls and negative for the “tail to tail” ones. As a consequence one should expect that the etching speed could be faster on domain boundaries with negative charge accumulation, i.e. the “tail to tail” walls. After etching begins at those places, there will be negative domain end surfaces exposed to acids, and the etching will proceed laterally. In summary we could expect as etching effect the formation of grooves on the surface of the sample, in places where negatively charged domain walls emerge. The longer is the etching time, the thicker and deeper will be the grooves. This could be a good method to reveal the negative walls of ODLN structures ending at the sample surface.

We submitted our sample to etching in the above mentioned acid mixture at 85°C over a period of 20 minutes. In Fig. 1 we present an optical microscope image of a region of the etched

surface. Figure 1a shows a general view of the etched domain structure. It may be noted a relatively regular sequence of domains, although the spacing in the left region becomes lower. By direct observation along the sample, and considering two opposite domains in each period, spacing of periods from 18 to 30 μm were detected. These spacings were also confirmed by laser light diffraction in different points of the surface. Some small regions presented a lack of periodic domain structure (top-left corner of Fig. 1a). Figure 1b shows a small region with higher magnification. More etched areas show greater roughness. However from this figure it is difficult to know the topography of the surface.

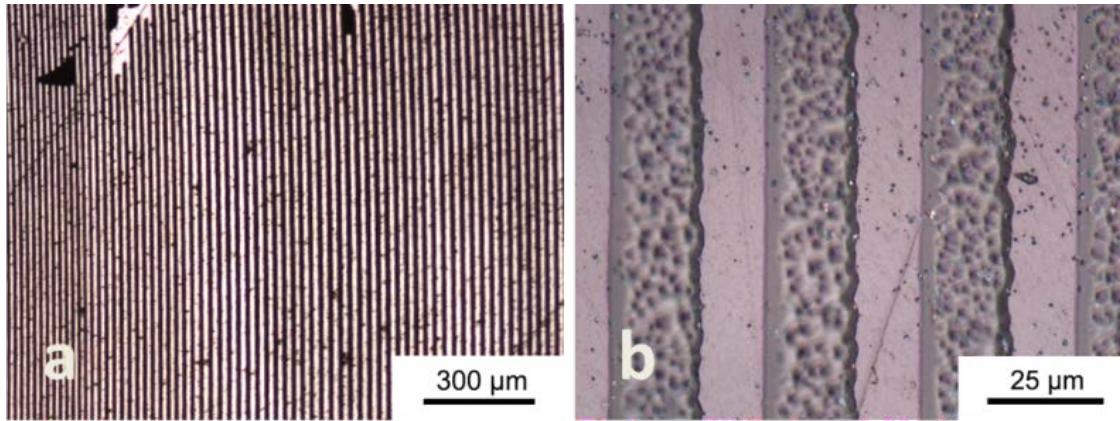


Figure 1.- Optical microscopy images of the etched sample. (a) A general view shown spacing regularity along the sample. (b) Detail of the etched grooves.

We completed the sample characterization measuring the topography of the sample by an atomic force microscope (AFM) model XE-100 Park System in non-contact mode. Fig. 2a shows a part AFM topographic image scanned in perpendicular to the etching grooves. In Fig. 2b we present the average topography plot obtained from image of Fig. 2a. Note that the valleys are formed from the negative domain ends walls. Considering the deeper point in one of these valleys, it can be observed that there is not a complete left-to-right symmetry, contrary to what

might be expected. This is explained because there is a slight surface disorientation. The c-axis of the crystal is not fully contained in the sample surface, and so does the polarization vector, \mathbf{P}_s . Therefore there is a small component of negative dipole ends on the right slope of each valley, while there is a positive component of dipole ends on the left slope. The extreme etching speed difference for negative to positive ends produce the asymmetry of the topography of the etched surface. This situation is sketched in Fig. 2c.

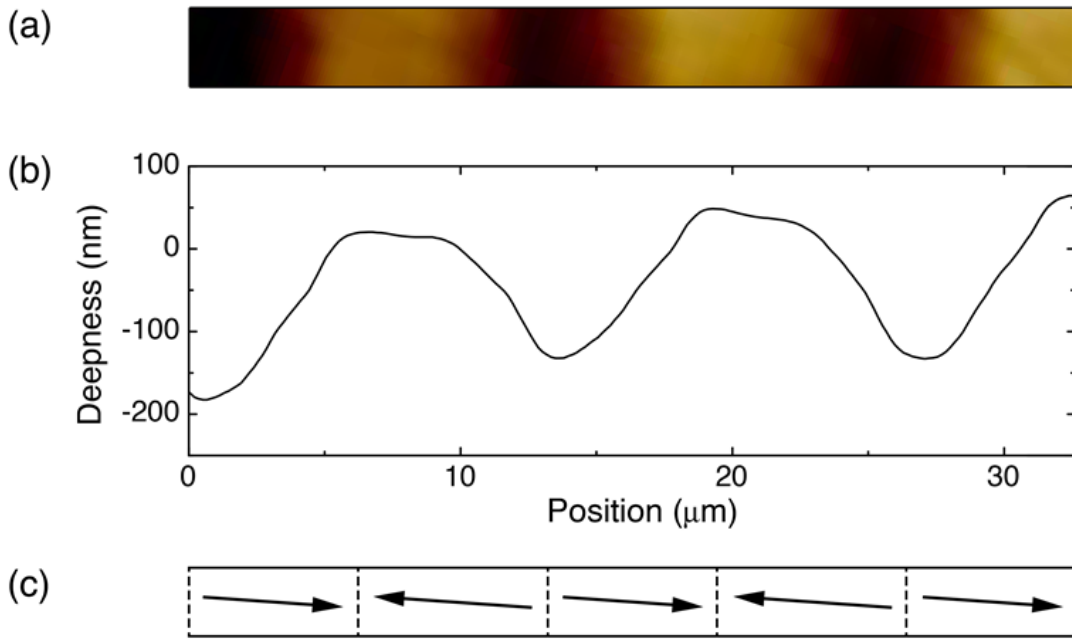


Figure 2.- (a) AFM topography image of the etched surface. (b) Topography plot of averaged data of Fig. 2a. (c) Sketch of a cut of the sample thickness shown the domain wall positions and the orientation of \mathbf{P}_s vectors inside each domain.

The slight tilting of the c-axis respect to the surface may affect the characteristics of nanoparticle trapping by the pyroelectric effect. Before starting the particles trapping experiments the sample was again polished to optical quality.

RESULTS

Trapping procedures. The pyroelectric coefficient, $p=(\partial P_s/\partial T)_T$, of lithium niobate near room temperature is $p=-4\cdot 10^{-9} \text{ Ccm}^{-2}(\text{°C})^{-1}$ [14]. The minus sign indicates that upon an increment of temperature the charge density on the positive domain surface decreases while on the negative one becomes less negative. Considering that the surface charge on the ambient exposed areas is initially neutralized by adsorbed species, such a temperature change leads to a negative charge on the positive domain ends while a positive charge is produced on the negative domain ends. If the temperature change occurs when the sample is in the air, changes in the adsorbed substances would lead to charge neutralization in a short time interval. However if there is a surface charge density when the sample is in a fluid with NPs in suspension, charge neutralization can occur by trapping the particles on the surface.

In the case of the ODLN sample, upon a temperature change, new uncompensated charge is expected at the lines of the domain walls emerging at the surface. Positive and negative alternating charge lines will appear. More particularly in the case of our sample, the slight disorientation of the surface could have consequences. Not only the wall lines at the surface will become charged. The domains pointing to the left in Fig. 2c have a small component of positive dipole ends at the surface and then all domain face will become negatively charged on rising temperature. The contrary will happen on the domains pointing to the right.

We considered two alternative procedures to produce surface charge and expose it to the NPs dispersed in a liquid. In the first one, sample was heated in air on a hot plate and rapidly immersed into the liquid remained at room temperature. The results may depend on the time interval that takes to introduce the sample in the liquid. During that small time the sample is cooling and the pyroelectric charge could be partially compensated by air moisture. The second

method consisted in keeping the liquid with NPs heated to a certain temperature above room temperature, e. g. 50°C. Then the cold sample is introduced in the hot liquid. In this circumstance the temperature change of the sample and thus the generation of the pyroelectric charge occurs inside the liquid. This second method seems to be more reproducible, and therefore we followed it in general. The only disadvantage is observed when using high vapor pressure and low boiling point liquids.

For our experiments on trapping and selective ordering of NPs on our ODLN structure we have used a variety of NPs and dispersing liquids. Among the particles we used metallic particles of silver and aluminum, uncovered and oleic acid covered. Lithium niobate NPs were considered as an example for nonmetallic NPs trapping. Respect to the dispersing liquids we can distinguish between non-polar ones such as hexane and heptane, and polar ones like water, oleic acid, acetone and ethanol. We proceeded as follows. A small amount of dry NPs were mixed in the dispersant and sonicated by 15 minutes. The mixture was kept to stand for half an hour to allow the sedimentation of the larger aggregates. After this time the upper half of the dispersion was taken for use in trapping.

Trapping of silver NPs: Trapping on the domain walls. In our sample the surface cuts the domain walls almost perpendicularly so that they appear as lines on the surface. In many of our trapping experiments we observed how the NPs appear aligned along the domain walls forming parallel straight lines. Very frequently the population of the walls is not uniform. In fact, they are in turn filled with more and less concentration of particles, as can be appreciated in Fig. 3a. In this figure we present the optical microscope image of a first example of trapping. We used in this case silver NPs of 40nm diameter dispersed in heptane. The mixture was heated to 70°C and the sample, initially at 25°C, was kept in the liquid during 30 s. The optical microscope cannot

distinguish individual particles but it is very useful to observe the results of the trapping and ordering of a number of them.

In Fig. 3b we present a graph of the dark pixels population integrated along the horizontal direction, what gives a good idea of particle population integrated along the direction of the domain walls. It is very clear that there are in turn walls highly saturated of particles and other less populated walls in between. Another feature of the image of Fig. 3a, also reflected in the graph, is related to the particles trapped on domain surface between walls. It is also clear that the domains below the highly populated walls present more trapped particles than the domain above. All these aspects will be discussed later.

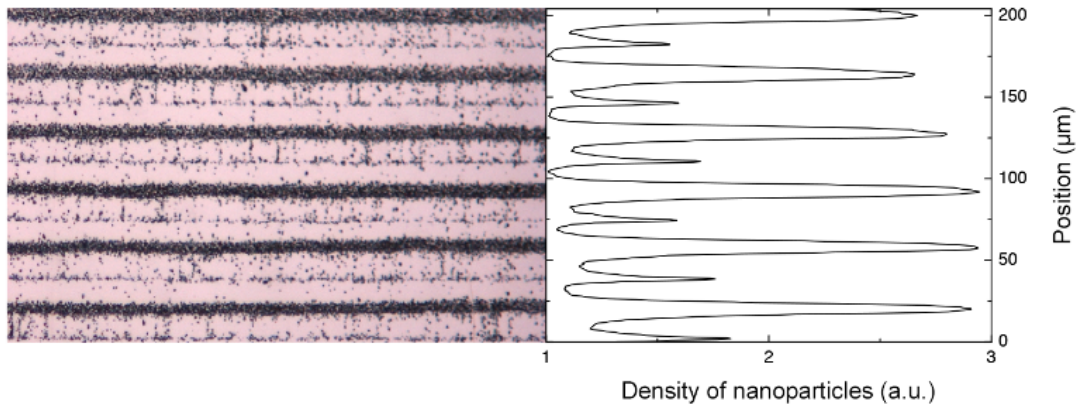


Figure. 3.- (a) Microphotography of silver particles trapped on the surface of the ODLN sample. (b) Graph of the averaged density of dark pixels as a function of the vertical direction. As particles are observed as dark points, this is a representation of NPs distribution in this direction.

In some occasions we observed that the particles are trapped only on alternate domain walls. This is the case shown in Fig. 4. A slight trapping on the domain above the populated walls is also observed. The domains below have practically no particles.

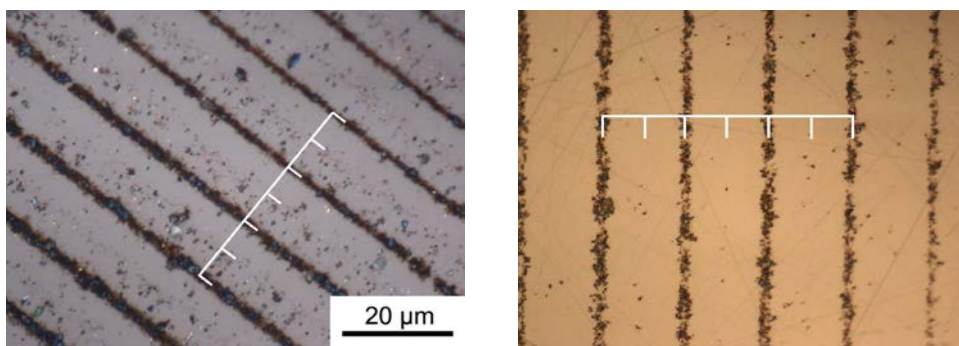


Figure 4.- Microphotographs of Ag NPs trapped mainly on alternate non-consecutive domain walls. The white line combs are to indicate the position of domain walls.

Trapping of silver nanoparticles: NPs chain formation. In many trapping experiments of Ag NPs on the ODLN surface we observed the formation of NPs chains. These chains are nearly straight and oriented perpendicularly to the domain wall lines. They appear connecting two consecutive walls. Then chains are about 10μ long. Note that consecutive walls are pyroelectrically charged with contrary sign charges. Considering the mean particle diameter of 40nm, many particles are involved in the formation of each chain. In Fig. 5a we show a microscopic picture of an experiment of weak trapping with the presence of chains. Additionally it can be observed that in this case plus and minus wall lines are populated with similar density of particles. In our experiments the formation of chains is a relatively common phenomenon. In cases of strong trapping they are observed in large quantities. Figure 5b shows a case of strong trapping with the presence of a high density of chains. In both figures, 5a and 5b, one can see that the chains preferably lie on alternate domains. This should be related to the slight disorientation that presents the surface of the sample, as was shown in the previous section.

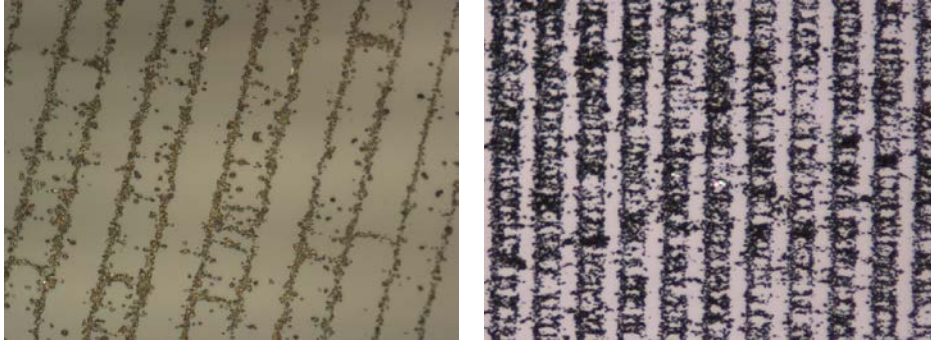


Figure 5.- (a) Microscope photograph of weak particles trapping shown the presence of some chains connecting consecutive domain walls. Most particles are trapped on the domain walls. (b) Microphotograph of a strong trapping of NPs shown a high density of chains between domain walls.

In fig. 6 we present SEM images of the NPs chains. With this higher magnification the structure of the chains is observed. In some cases the chain is not completed from one domain wall to the next one. In this figure the positions of domain walls is indicated using dotted lines. Other features of the trapping can be also observed in this figure.

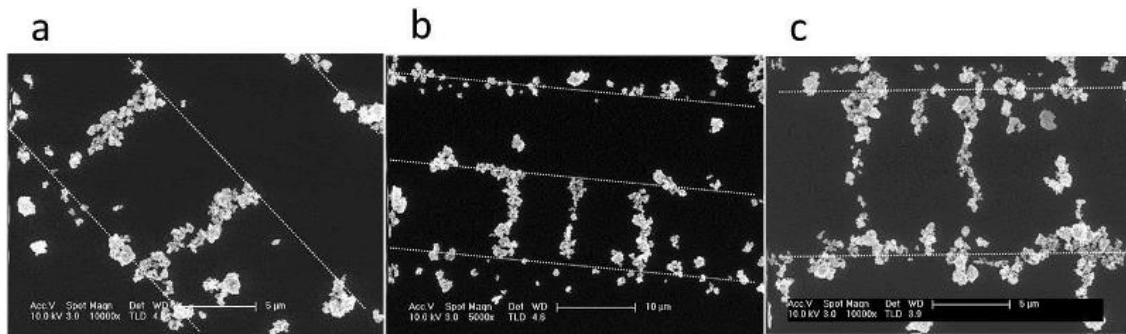


Figure 6.- (a to c) SEM images of trapped NPs forming chains. The dot lines are included as a help for the eye to show the position of domain walls.

Sometimes we have observed that the NPs are trapped exclusively in chain formation. In these cases we did not observe preferential entrapment on the border between domains. This is shown

in Figure 7. It can be seen, as in above presented cases, that chains very preferentially lie on alternate domains.

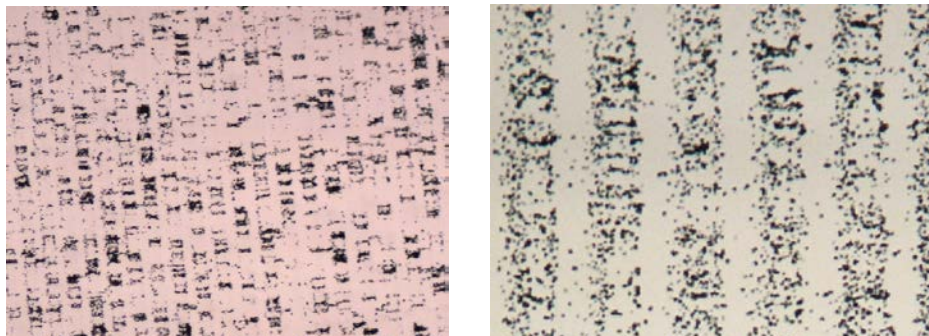


Figure 7.- Two examples of Ag NPs trapping where preferential accumulation of particles on the domain wall is not observed. Note that there is a magnification factor of 5 between both images.

In order to check the adhesion of the particles to the surface of the sample, we performed experiments of contact transfer of already trapped particles to a tape. The proportion of transferred particles was very high and the order pattern remained. This could be interesting for applications of NPs structures requiring other substrates.

We have also performed similar experiments of trapping but using NPs dispersed in polar liquids. We used oleic acid, distilled water, acetone and ethanol. The procedure was the same as in the experiments performed with NPs dispersed in heptane and hexane whose results we have exposed above. Conversely, in the experiments with polar liquids we did not observe any trapping of NPs.

Trapping of LiNbO_3 NPs. In order to investigate the pyroelectric trapping of non-metallic particles on the ODLN structure we used lithium niobate (LN) NPs. These NPs were produced in our lab from precursors following the process described in detail in ref. 19. X-ray powder analysis indicated a mean particle diameter of about 40nm. The dispersing fluid was Heptane.

Two examples of LN NPs trapping results are shown in Fig. 8. Left picture presents particles mainly trapped along alternate domain walls, in a similar way as that observed for Ag particles.

The picture on the right corresponds to a case of stronger trapping. Here we see first that in addition to the walls heavily populated of NPs, intermediate walls are also weakly populated. Secondly we see the emergence of some cross chains (left side of image). Finally we can see that on the walls more populated of trapped NPs, they appear more dispersed than in the case of the silver particles above presented.

As in the preceding cases, pyroelectric trapping was not successful when the particles were dispersed in polar liquids such as water, ethanol or oleic acid.

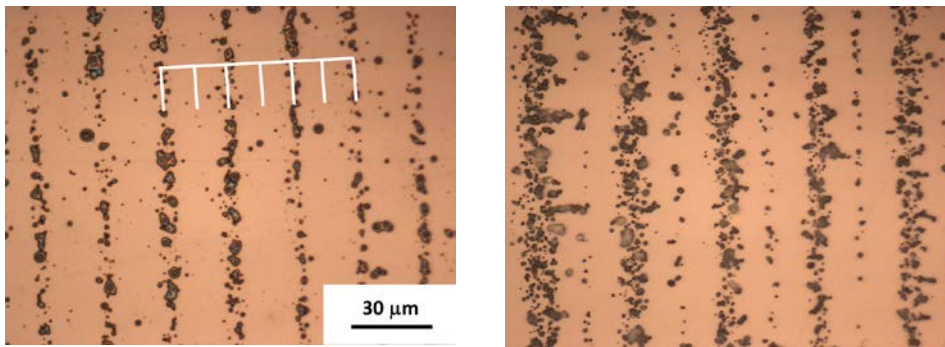


Figure 8.- Two examples of pyroelectric trapping of lithium niobate NPs on the ODLN material. The white line comb is to indicate the position of the domain walls.

DISCUSSION AND CONCLUSIONS

Possible forces acting in the trapping process are: dielectrophoretic forces (DPF) on polarized neutral NPs, and electrophoretic forces on previously charged PNs. Both forces could act together on weakly charged particles. Temperature changes produce pyroelectric charges at the domain wall surface lines on the surface of our ODLN sample. Due to the domain structure the sign of charges are alternated between consecutive domain wall lines. Additionally, the surface

of each domain will be weakly charged due to the small disorientation of the surface respect to the c-axis of the crystal. Also alternately, the surface of a domain will be positively charged while that of the next one will be negatively charged. Under this charge distribution, and its associated electric field, the NPs trapping will occur.

Assuming a given surface charge density on the crystal, the trapping of charged particles of opposite sign is more effective than the trapping of neutral particles. Trapping of charged particles is mainly due to the electrophoretic force between charges of opposite sign. One has also to consider that these particles will be polarized resulting in an additional attractive force of dielectrophoretic character. On the other hand, neutral particles will be polarized due to the electric field of the sample charge, and therefore will suffer an attractive force of dielectrophoretic character exclusively. Clearly this force is weaker than that acting on the charged particles¹⁵. In addition, in the hypothetical event of equal density of charged and uncharged particles, and assuming that both types of particles have equal sizes and average speeds, relatively greater proportion of charged particles will be trapped.

Selective trapping of NPs on the walls charged with a specific sign, and the absence of trapping on the walls of opposite sign, is the undeniable proof that all the particles were charged with the opposite sign to the wall line charge. The force acting in this case is the electrophoretic one. We observed this situation in metallic Ag NPs trapping, Fig. 4, as well as with lithium niobate non-metallic ones, Fig. 8a. In certain cases additionally to this trapping on the wall lines we observed a slight trapping on the domain surface at one side of the wall. This will correspond to the domain weakly charged of the same sign as the populated wall. This is the case of figure 4a.

Other times it is seen that all lines of domain wall trap particles, but with alternating high and low NPs population. This is well evident in figure 4. In such a case we have to conclude that the trapping was done in the presence of a mixture of charged and neutral particles. The charged particles trap on the walls of opposite sing by electrophoretic forces. On the other hand neutral particles are polarized by the charge on the surface of the sample. They will then be trapped on domain wall lines of both sings by means of dielectrophoretic forces. All the charged particles must have charge of the same sing. The existence in the liquid of particles charged with both charge sings should be discarded because they attract joining together before being trapped.

In the case shown in figure 5 consecutive domain wall lines seem to be almost equally populated. This must be attributed to that in this case all the particles are neutral. Trapping there is exclusively due to dielectrophoretic forces.

The formation of chains of particles is definitely due to dielectrophoretic forces between neutral or weakly charged particles. In fact, charged particles repel each other and can never link together. A chain starts when a neutral particle is polarized by a charged domain wall and becomes trapped therein. A new neutral particle approaching the previous one in the fluid is in turn polarized by the uncompensated charge of the already trapped particle, and is trapped on it. The process of trapping on the last trapped particle continues many times forming the chain. In our observations the chains finally lie on a domain surface, pointing perpendicularly to the domain walls, and mostly ending on the wall next to the starting one. The formation of chains due to dielectrophoretic forces in a pyroelectric field has been previously observed with carbon NPs dispersed in a polymer solution²⁰.

Several pictures of Ag NP trapping presented in this paper show chains. In some of them the relative number of chains is low as in Figs. 4a and 5a. In figure 5b the density of chains is very

high, combined with a higher population of NPs on one of the alternate domain walls. In this case we can conclude that some of the particles were charged, but many of them were neutral, or very weakly charged, forming the chains. It is noticeable the case of figures 7a and 7b, for which the particles form chains only, not showing greater entrapment on domain boundaries. Here the particles seem to be uncharged.

One aspect still not commented is that in all cases the chains very preferentially lie on alternate domain surfaces. Very few chains can be found on the other domains. As stated above, the only difference between the surfaces of consecutive domain is the weak charge densities alternating the sign from a domain to the next one. The chains prefer to lie on a surface of a determined charge sign. We may very tentatively suggest as explanation of this behavior that the particles forming the chain could be slightly charged.

SEM images present in Fig. 7 show that the chains are not formed by one single line of individual particles but by a large number of particles forming clusters. Sometimes the chains are not continuous from one wall to the next.

In ODLN pyroelectric trapping chains are not exclusive of metallic NPs. Lithium niobate NPs chains are also observed as in Fig. 8b. They also seem to lie preferentially on one of the domain surfaces charged with a particular sign of charge. So far we are not able to know the sign of the charge preferred.

We have not succeeded in pyroelectric trapping of NPs when the particles were dispersed in polar liquids, for example water, oleic acid, ethanol, etc. In these cases the liquid molecules seem to screen the electric fields close to the surface, reducing the trapping forces below the value needed for trapping.

In conclusion we were able to trap NPs on selective sites of the surface of an ODLN sample charged using the pyroelectric effect. Up to our knowledge this is the first reported study of such trapping. The particular structure of the sample provides a surface having alternate lines of opposite charge. This is quite interesting in order to distinguish whether the NPs dispersed in the fluid are neutral or charged. The charged NPs in a dispersion will have all of them the same charge sign. Then they will very preferentially trap on alternate domain wall surface lines. This has been observed in some trapping cases. In contrast, neutral NPs will not have preference by a particular charge sign position. In this case, all consecutive wall lines are expected to be equally populated by trapped NPs. The force in this case will be of dielectrophoretic nature. A mixture of charged and neutral NPs in the fluid will produce trapping of NPs on all the wall lines but with alternated population density. This case has been observed frequently. A characteristic figure of trapping of uncharged particles is the formation of linear chains of NPs bound by dielectrophoretic forces. This has also been observed very frequently with metallic as well as with non-metallic NPs.

In none of our experiments we did any process to charge the NPs purposely. Often the particles were electrically charged during normal handling. This indicates the great ease with which the NPs get charged. Our pyroelectric trapping on ODLN structures could be a valuable test to check the charging state of particles dispersed in a liquid. Further efforts will be made to explore whether it is possible, and under what conditions (such as pH values), the trapping on the surface of structures ODLN of NPs dispersed in polar liquids. This could be of major interest for biomedical applications. Finally, the particular ferroelectric domain structure of ODLN crystals could be also interesting for self-structuring of polymer layers due to charge sensitive wettability of solved polymers, as it has been already studied on PPLN structures^{21,22}.

AUTHOR INFORMATION

Corresponding Author

*Tel. +34914975026. Email: luis.arizmendi@uam.es

Notes

Authors declare no competing financial interest.

ACKNOWLEDGEMENTS

This work has been supported by the Spanish Ministerio de Economía y Competitividad under grant ref.: MAT2014-57704-C3-1-R. One of the authors (A. Gallego) acknowledges the Spanish Ministerio de Educación, Cultura y Deporte for a collaboration fellowship.

REFERENCES

- [1] Ashkin, A.; Dziedzic, J.M.; Bjorkholm, J.E.; Chu, S. Observation of a single-beam gradient force optical trap for dielectric particles. *Opt. Lett.* **1986**, *11*, 288–290.
- [2] Jones, T. B. *Electromechanics of particles*; Cambridge University Press: Cambridge, U. K., 1995.
- [3] Zborowski, M.; Chalmers, J. J. *Magnetophoresis: Fundamentals and Applications*; Wiley Encyclopedia of Electrical and Electronics Engineering. 1–23, 2015.
- [4] Chiou, P. Y.; Ohta, A. T.; Wu, M. C. Massively parallel manipulation of single cells and microparticles using optical images. *Nature* **2005**, *436*, 370–372.
- [5] Eggert, H. A.; Kuhnert, F. Y.; Buse, K.; Adleman, J. R.; Psaltis, D. Trapping of dielectric particles with light-induced space-charge fields. *App. Phys. Lett.* **2007**, *90*, 241909.
- [6] Villarroel, J.; Burgos, H.; García-Cabañes, A.; Carrascosa, M.; Blázquez-Castro, A.; Agulló-López, F. Photovoltaic versus optical tweezers. *Opt. Express* **2011**, *19*, 24320–24330.

- [7] Grilli, S.; Ferraro, P. Dielectrophoretic trapping of suspended particles by selective pyroelectric effect in lithium niobate crystals. *Appl. Phys. Lett.* **2008**, *92*, 232902.
- [8] Grilli, S.; Coppola, S.; Nasti, G.; Vespini, V.; Gentile, G.; Ambrogi, V.; Carfagna, C.; Ferraro, P. Hybrid ferroelectric–polymer microfluidic device for dielectrophoretic self-assembling of nanoparticles. *RSC Adv.* **2014**, *4*, 2851–2857.
- [9] Carrascosa, M.; García-Cabañes, A.; Jubera, M.; Ramiro, J. B.; Agulló-López, F. LiNbO₃: A photovoltaic substrate for massive parallel manipulation and patterning of nano-objects. *Appl. Phys Rev.* **2015**, *2*, 040605.
- [10] Räuber, A. Chemistry and physics of lithium niobate, chapter 7 in *Current Topics in Materials Science*. Ed. Kaldis, E. North-Holland Pub. Co.: Amsterdam, Holland 1978.
- [11] Arizmendi, L. Photonic applications of lithium niobate crystals. *Phys. Stat. Sol. a* **2004**, *201*, 253–283.
- [12] Bermúdez, V.; Serrano, M.D.; Dutta, P.S.; Diéguez, E. Opposite domain formation in Er-doped LiNbO₃ bulk crystals grown by the off-centered Czochralski technique. *J. Cryst. Growth* **1999**, *203*, 179–185.
- [13] Zhu, Ming, N-b. High-frequency resonance in acoustic superlattice of LiNbO₃ crystals. *Appl. Phys. Lett.* **1988**, *53*, 2278–2280.
- [14] Savage, A. Pyroelectricity and Spontaneous Polarization in LiNbO₃. *J. Appl. Phys.* **1966**, *37*, 3071.
- [15] Mokřý, P.; Marvan, M.; Fousek, J. Patterning of dielectric nanoparticles using dielectrophoretic forces generated by ferroelectric polydomain films, *J. Appl. Phys.* **2010**, *107*, 094104.

- [16] Ferraro, P.; Grilli, S. Pyroelectric effect inducing trapping of particles on periodically poled lithium niobate crystals. *Proc. of SPIE* **2008**, 6988, C1–C7.
- [17] Bermúdez, V.; Serrano, M.D.; Dutta, P.S.; Diéguez E., On the opposite domain nature of Er-doped lithium niobate crystals. *Sol. State Commun.* **1999**, 109, 605–609.
- [18] Nassau, K.; Levinstein, H.J.; Loiacono, G.M. Ferroelectric lithium niobate. 1. Growth, domain structure, dislocations and etching. *J. Phys. Chem. Solids* **1966**, 27, 983–988.
- [19] Knabe, B.; Schütze, D.; Jungk, T.; Svete, M.; Assenmacher, W.; Mader, W.; Buse, K. Synthesis and characterization of Fe-doped LiNbO₃ nanocrystals from a triple-alkoxide method. *Phys. Status Solidi a* **2011**, 208, 857–862.
- [20] Gennari, O.; Grilli, S.; Coppola, S.; Pagliarulo, V.; Vespini, V.; Coppola, G.; Bhowmick, S.; Gioffré, M.A.; Gentile, G.; Ambrogio, G.; Cerruti, P.; Carfagna, C.; Ferraro, P. Spontaneous Assembly of Carbon-Based Chains in Polymer Matrixes through Surface Charge Templates. | *Langmuir* **2013**, 29, 15503–15510.
- [21] Grilli, S.; Vespini, V.; Ferraro, P. Surface-Charge Lithography for Direct PDMS Micro-Patterning. *Langmuir* **2008**, 24, 13262–13265.
- [22] Xi, X.; Zhao, D.; Tong, F.; Cao, T. The self-assembly and patterning of thin polymer films on pyroelectric substrates driven by electrohydrodynamic instability. *Soft Matter*, **2012**, 8, 298–302.

TOC Graphic

